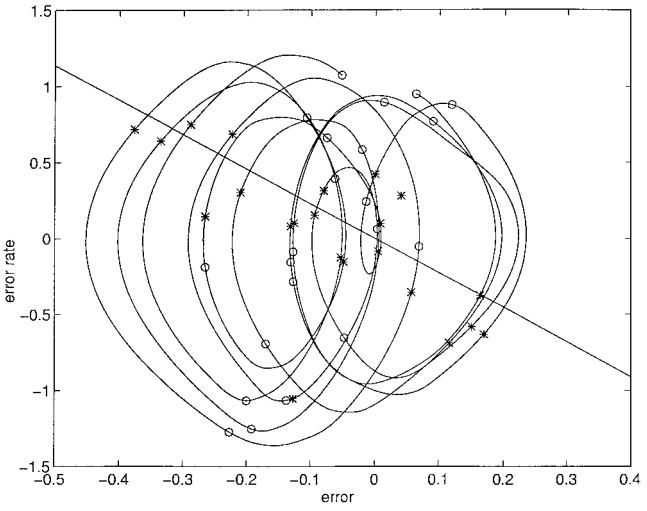

Fig. 9 Modified phase plane and switching line.

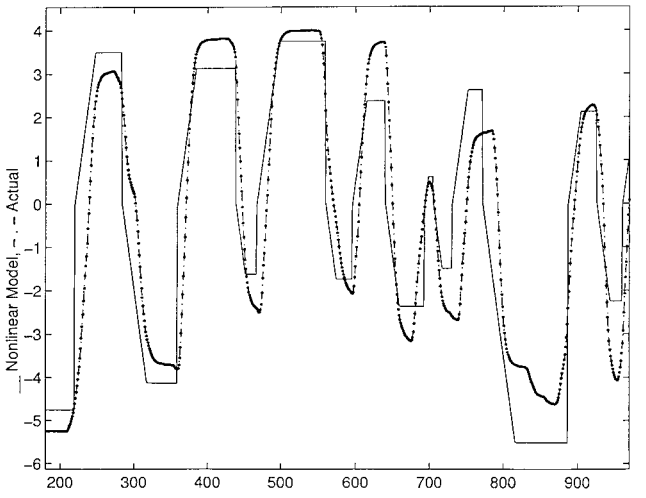

Fig. 10 Comparison between model and experimental control.

V. Conclusions

A novel structure of a human operator in a control loop has been introduced, modeling manual control behavior in situations where such control requires a switching strategy. The model is based on an adaptive delayed relay structure with a linear switching line. Model parameters were obtained from a limited experimental database. Although preliminary in nature, the model shows performance consistent with the experimental data; the generality of the approach of course needs additional validation, and it may be limited to situations where operator control pulsing is clearly excited by appropriate input to the closed-loop system. The model identification parameters (k, γ, τ) appear candidate parameters to evaluate different operators' capabilities and training levels.

Acknowledgments

This work was partially supported by the Italian Ministry of University, Scientific, and Technological Research under Grant MURST 40% "Control Engineering." The authors wish to thank Giovannoni and Folgarait for their valuable help in setting up the simulation facility and performing the experimental work.

References

[1]AGARD/NATO, "Advances in Flying Qualities," AGARD-LS-157, Lecture Series, May–June 1988.

[2]McRuer, D. T., and Krendel, E. S., "Human Dynamics in Man-Machine Systems," *Automatica*, Vol. 16, 1980, pp. 237–253.

[3]Hess, R. A., "Structural Model of the Adaptive Human Pilot," *Journal of Guidance, Control, and Dynamics*, Vol. 3, No. 5, 1980, pp. 416–423.

[4]Innocenti, M., "The Optimal Control Pilot Model and Application," AGARD LS-157, Lecture Series, Lecture No. 8, May–June 1988.

[5]Davidson, J. B., and Schmidt, D. K., "Modified Optimal Control Pilot Model for Computer-Aided Design and Analysis," NASA-TM-4384, 1992.

[6]MacAdam, C., "Application of an Optimal Preview Control for Simulation of Closed Loop Automobile Driving," *IEEE Transactions on Systems, Man, and Cybernetics*, Vol. 11, June 1981, pp. 393–400.

[7]Sheridan, T. B., and Ferrell, W. R., *Man-Machine Systems: Information, Control, and Decision Models of Human Performance*, Massachusetts Inst. of Technology Press, Cambridge, MA, 1974.

[8]Innocenti, M., Balluchi, A., and Balestrino, A., "New Results on Human Operator Modelling During Nonlinear Behavior in the Control Loop," American Control Conference ACC97, July 1997.

[9]Utkin, V., *Sliding Modes and Their Application in Variable Structure Systems*, MIR, Moscow, 1978.

[10]Slotine, J.-J. E., and Li, W., *Applied Nonlinear Control*, Prentice–Hall, Upper Saddle River, NJ, 1991.

Experiments on Space Robot Arm Path Planning Using the Sensors Database, Part II

Toshiaki Iwata*
Electrotechnical Laboratory, Ibaraki 305-8568, Japan
Seiya Ueno†
Yokohama National University, Yokohama 240-8501, Japan
and
Hiroshi Murakami‡
Electrotechnical Laboratory, Ibaraki 305-8568, Japan

Introduction

THE orientation of a free-flying space robot is disturbed by the arm movement. However, the space robot can simultaneously control the orientation of its main body and arm position using only arm motion due to its nonholonomic constraints.[1–4] We have presented path-planning methods such as breadth-first search and A^* search, using a sensor-motion database, which are not model-based methods but sensor-based ones.[1] However, the breadth-first search required a long time to determine the path, and A^* search did not always indicate the shortest solution or did not find the path at all. These methods yielded the path only after a successful search, so that the search could not be terminated halfway. In actual situations, because the tasks of the space robot will be composed of a series of planned motions, the paths should be short and planned in a short time even though they may not be the shortest possible. The genetic algorithm (GA), which uses the same database as that of the previous search methods, yields a temporary path in a short time. Furthermore, because the database is specific to discrete joint angles, it is not possible to accommodate arbitrary continuous values. This presents a serious problem. Therefore, we approximate the relationships between sensor states and robot motions in the database using a formula and use optimal control techniques with the formula to deal with continuous joint angle values.

Path-Planning Methods

The space robot situation considered and the database used in the experiments are the same as those shown in Figs. 1 and 2 of Ref. 1

Received 18 December 1998; revision received 16 December 1999; accepted for publication 7 February 2000.

*Senior Researcher, Frontier Technology Division, 1-1-4 Umezono, Tsukuba. Senior Member AIAA.

†Associate Professor, Division of Artificial Environment and Systems, 79-5 Tokiwadai, Hodogaya-ku. Member AIAA.

‡Senior Researcher, Frontier Technology Division, 1-1-4 Umezono, Tsukuba.

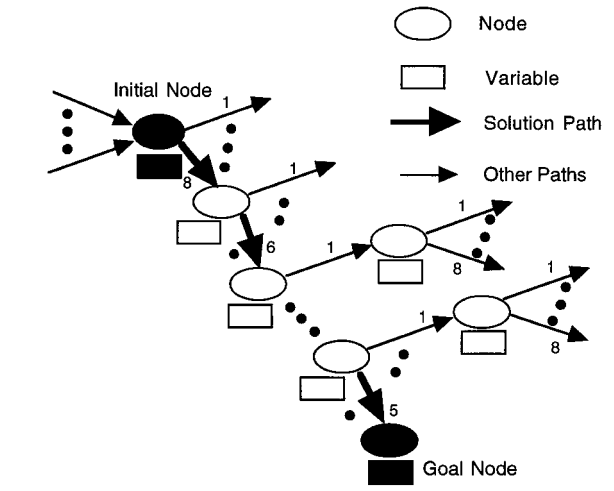

a) Search method

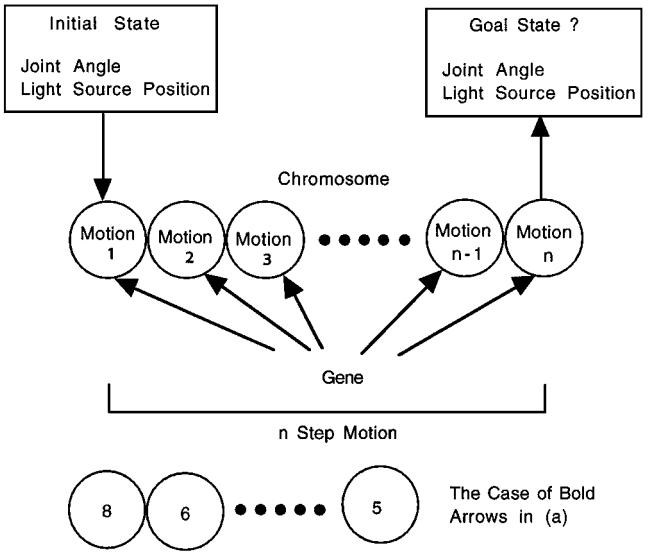

b) Composition of chromosome

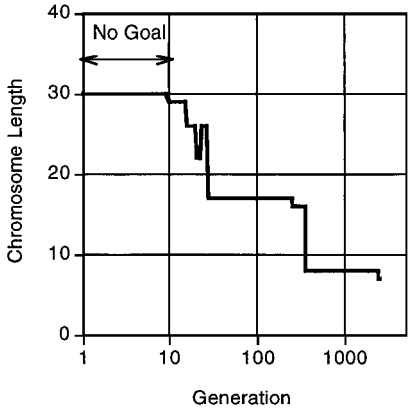

c) Evolution process

Fig. 1 Process of GA.

(symbols are also the same). Using the database, we searched the solution from $q_1 = 195$ deg, $q_2 = -75$ deg, and $p_1 = p_2 = 255$ to $q_1 = 15$ deg, $q_2 = -75$ deg, and $p_1 = p_2 = 255$, which is also the same as that of Ref. 1. Although we used the breadth-first search and A^* search to find the path, they have drawbacks, as pointed out in the Introduction. To overcome those drawbacks, we propose two methods: GA and optimal control.

GA

First, the arrows, that is, state transitions, in Fig. 3 of Ref. 1 were numbered for each node (shown here in Fig. 1a). The string of arrow

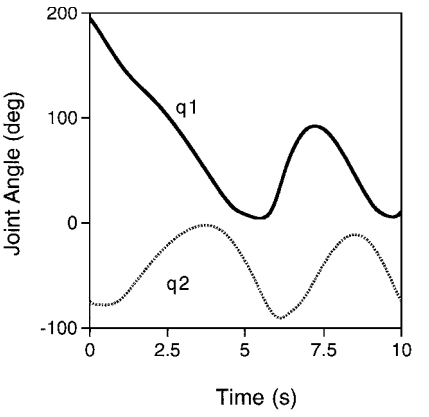

a) Joint angles

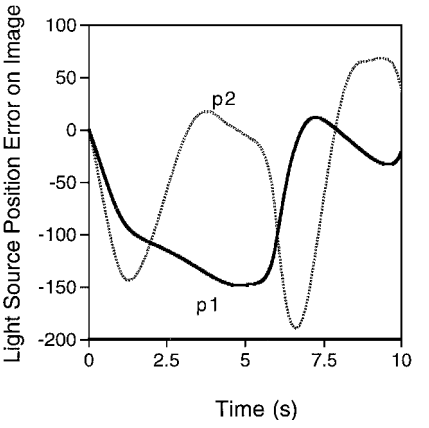

b) Light source position error during motion

Fig. 2 Cyclic motion resulting from optimal control.

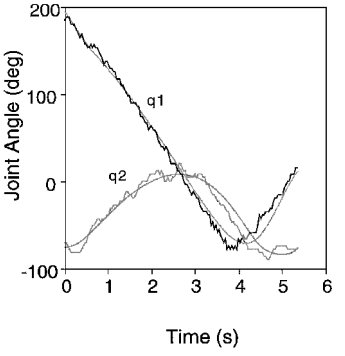

a) Joint angles

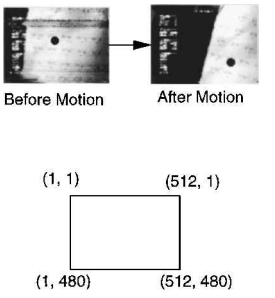

b) Camera images

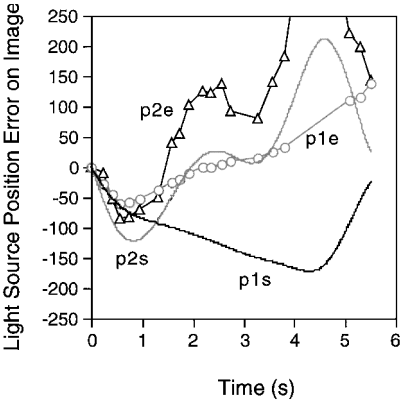

c) Light source position error during motion

Fig. 3 Optimal control results.

numbers indicates a series of robot motions. If the arrow number is used as an allele, that is, the value of a gene, of a chromosome of length n, that is, the chromosome is composed of n genes, then the chromosome represents an n-step motion of the robot (Fig. 1b). For instance, the chromosome marked in Fig. 1a (bold arrows) is expressed in Fig. 1b. In an ordinary GA, the length of a chromosome is fixed. However, in our case, the chromosome length, that is, number of motion steps, is variable. To use the GA for finding the shortest path, we define the *fitness* as

$$fitness = (1/length) + g \tag{1}$$

where *length* is the chromosome length and g is 0.3 if the final state, that is, the joint angles and the light source position on the image, is the goal; otherwise g is 0. The goal state should be given as discrete joint angles (the node values) and the permissible range of the charge-coupled device camera output as the node variable. If the range is narrow, the search might fail, and so we set the range within ±100 pixels, that is, $155 < p_1$ and $p_2 < 355$. The larger the fitness, the better the chromosome.

There are two kinds of operations in GA: crossover and mutation. Two parents yield one child as a result of crossover. The two parents are selected by the roulette method in which the parent chromosome is chosen to be proportional to the fitness value. The same states, that is, the same joint angles and the same light source position on the image, in both chromosomes are selected, and the shorter segments of the parent chromosomes are connected to yield a new chromosome. The probability of mutation for a chromosome that reaches the goal state is lower than that for a chromosome that does not reach the goal state (40%) because it is undesirable to lose a chromosome that reaches the goal state. Because mutation affects all states after it has occurred, all genes after the point of mutation are changed.

The GA uses the following parameters. The number of chromosomes in the pool is 30, the maximum length of the chromosome is 30, the probability of mutation is 0.5, that is, 0.5 for a chromosome that does not reach the goal state, and 0.5×0.4 for a chromosome that reaches the goal state, and the total number of generations is 2,500. The evolution process is shown in Fig. 1c. In the 10th generation, a chromosome that reaches the goal state appears. The length of the chromosome is 29 genes. After that, the length shortens, and finally, a chromosome with seven genes appears in the 2,436th generation. The seven-step motion, which results in the same motion as that obtained by the breadth-first search, was acquired.[1] This means that the GA also yielded the shortest path. However, the GA cannot judge whether this path is the shortest or not a priori because the GA does not guarantee the optimal solution and only evolves the chromosomes using the fitness values.

In the case of breadth-first search, 93,452 nodes were searched before the path was found, and no other candidate path existed. In the case of A^* search, we found the path after a 282-node search; however, the number of searched nodes depends on the searched path, and in some cases, a path is not found or, if found, is very long. On the other hand, in the case of the GA, we found the shortest path after $30 \times 2{,}436 = 73{,}080$ nodes were searched. Even though the GA does not require the use of the pruning technique, which consumes considerable memory and time, it does not seem to have an advantage compared to breadth-first search. Moreover, the number of searched nodes depends on the searched path and the parameters of the algorithm, including the random generator in the program. However, in general, the GA arrived at a temporary solution, such as a more-than-8-step path, at an early stage. Therefore, even if we stop the search halfway, the GA provides a temporary solution at that time. This is an important property for actual use. If a path of less than 10 steps is admissible, only $30 \times 356 = 10{,}680$ nodes are searched and the 8-step path is obtained if we use the same parameters.

Optimal Control Techniques

Previous methods, including breadth-first search, A^* search, and the GA, cannot deal with continuous joint angles. This is the critical problem in their actual use. Therefore, we should extend the method to enable the use of continuous joint angles. A method using optimal control techniques is proposed. First, we approximate the database using polynomial and trigonometric expressions. Basically, because there are eight types of transitions (control inputs, ac_1 and $ac_2 = \pm 30$ or 0 deg) for each joint configuration, equations containing eight unknown coefficients are reasonable. Therefore, we use the following formulas to approximate the database relations:

$$f_i = a_{i1}u_1 + a_{i2}u_2 + a_{i3}u_1^2 + a_{i4}u_1u_2 + a_{i5}u_2^2 + a_{i6}u_1^2u_2 + a_{i7}u_1u_2^2 + a_{i8}u_1^2u_2^2 \tag{2}$$

where $u_1 = ac_1$ and $u_2 = ac_2$ are inputs, $f_i = dp_i$, and a_{ij} ($i = 1$ and 2, $j = 1, \ldots, 8$) are unknown coefficients that are functions of q_1 and q_2. After solving the preceding equations for each joint configuration, we set a_{ij} as

$$a_{ij} = b_{1ij} + b_{2ij}\sin q_1 + b_{3ij}\sin q_2 + b_{4ij}\cos q_1 + b_{5ij}\cos q_2 + b_{6ij}\sin q_1 \sin q_2 + b_{7ij}\sin q_1 \cos q_2 + b_{8ij}\cos q_1 \sin q_2 + b_{9ij}\cos q_1 \cos q_2 \tag{3}$$

and solve b_{kij} ($k = 1, \ldots, 9$, $i = 1$ and 2, $j = 1, \ldots, 8$) using the least-squares method. Using these formulas, we can extrapolate the relation beyond the range of the database.

Furthermore, the cost function to be minimized is set as

$$L = \int_0^{10} \left(u_1^2 + u_2^2\right) \mathrm{d}t \tag{4}$$

The terminal time is fixed as 10 s. Because the quadratic form in an angular velocity vector with an inertia matrix represents the kinematic energy of a system, this function is related to the energy supplied by joint motors. Therefore, the minimization of Eq. (4) provides the near-minimum energy-consumption path. We use the sequential conjugate gradient-restoration algorithm (SCGRA)[5] first for the large-error phase and the modified quasi-linearization algorithm (MQA)[6] for the small-error phase.

In the planned path using Eqs. (2–4), the joint angle q_2 is outside of the physical mobility range, that is, $q_2 < -90$. It is impossible to position the joint at such an angle, so that this motion is not feasible. Therefore, we introduce a penalty function in Eq. (4), that is,

$$L = \int_0^{10} \left(u_1^2 + u_2^2 + f_{p2}\right) \mathrm{d}t \tag{5}$$

where f_{p2} is a penalty function adopted to satisfy the range of q_2 and to prevent movement beyond −90 deg,

$$f_{p2} = \begin{cases} 0 & (x_2 \geq x_{2c}) \\ w_2\left(\dfrac{x_2 - x_{2c}}{x_{2m} - x_{2c}}\right)^2 & (x_2 < x_{2c}) \end{cases}, \tag{6}$$

where $w_2 = 1$, $x_2 = q_2$, $x_{2c} = -75$ deg, and $x_{2m} = -90$ deg. Although the planned path is outside the database range of q_1, this path is feasible, and so the path is used in the experiments. However, it might cause error. Therefore, we attempt to plan a path within the database range. To do so, we again introduce the penalty function for q_1, which is the same as Eq. (6),

$$f_{p1} = \begin{cases} 0 & (x_1 \geq x_{1c}) \\ w_1\left(\dfrac{x_1 - x_{1c}}{x_{1m} - x_{1c}}\right)^2 & (x_1 < x_{1c}) \end{cases}, \tag{7}$$

where $w_1 = 2$, $x_1 = q_1$, $x_{1c} = 15$ deg, and $x_{1m} = 0$ deg, and the cost function is

$$L = \int_0^{10} \left(u_1^2 + u_2^2 + f_{p1} + f_{p2}\right) \mathrm{d}t \tag{8}$$

The planned path and the motion of the light source position are shown in Fig. 2. This path seems to be a cyclic motion of the arm.

Some researchers have pointed out that the cyclic motion of the arm is effective for controlling both arm shape and body orientation.[2–4] Our result verifies this property of a space robot when the mobility ranges of the joint angles are limited.

Experiments

The same experiment as Ref. 1 was performed. Because the path planned by the GA was the same as the breadth-first search in Ref. 1, the result is not described here.

In the case of optimal control, because the experiment is limited to a total time of 10 s, the path obtained using Eqs. (3–5) should be compressed to about 5.5 s. Moreover, because this robot cannot control the joint angles and angular velocities continuously, 20 discrete points from the path were used to execute the experiment. The results of joint motion are shown in Fig. 3a. The dotted lines indicate ideal compressed paths, and solid lines indicate the actual motions. They are in good agreement. In Fig. 3, the origin of time is taken as the time of initial robot motion. Figure 3b shows the camera images of the grid graph paper before and after the motion. The light source positions, represented by black circles, are slightly different, even though they should be the same. In Fig. 3c, (p_{1e}, p_{2e}) indicates the experimental results for the motion of the light source position effect on the image, and (p_{1s}, p_{2s}) represents the simulated results: p_2 motions are in good agreement, whereas p_1 motions are not.

There are four possible causes of error. The first is model inaccuracy. The second is error of the database itself. These have been explained previously.[3] However, the third and fourth possibilities are peculiar causes related to optimal control. The third possibility is the assumption of $\mathrm{d}p_i = \dot{p}_i$. Here $\mathrm{d}p_i$ was measured by moving the joints ±30 deg/s for 1 s, whereas $\dot{p}_i$ is the velocity of the image motion in a pixel, where infinitesimally small motion during an infinitesimally small time period is assumed. Obviously, the assumption of $\mathrm{d}p_i = \dot{p}_i$ is in error. The fourth possibility is motion beyond the database. The joint angle q_1 moves in the negative range during the motion, which is out of the database range. This might result in an error.

Conclusions

Based on the results, the following general conclusions can be made.

1) The merit of GA lies in finding a temporary path at an early stage.

2) The merit of using optimal control techniques lies in the ability to deal with continuous joint angle values.

3) Results verify the property of cyclic motion of the arm for control when the ranges of joint angles are limited.

Acknowledgments

This work is supported by the New Energy and Industrial Technology Development Organization through the Japan Space Utilization Promotion Center in the program of the Ministry of International Trade and Industry.

References

[1]Iwata, T., Kodama, K., Numajiri, F., and Murakami, H., "Experiments on Space Robot Arm Path Planning Using the Sensors Database," *Journal of Guidance, Control, and Dynamics*, Vol. 22, No. 4, 1999, pp. 573–578.

[2]Longman, R. W., "The Kinematics and Workspace of a Satellite-Mounted Robot," *Journal of Astronautical Sciences*, Vol. 38, No. 4, 1990, pp. 423–440.

[3]Nakamura, Y., and Suzuki, T., "Planning Spiral Motions of Nonholonomic Free-Flying Space Robots," *Journal of Spacecraft and Rockets*, Vol. 34, No. 1, 1997, pp. 137–143.

[4]Yamada, K., and Yoshikawa, S., "Feedback Control of Space Robot Attitude by Cyclic Arm Motion," *Journal of Guidance, Control, and Dynamics*, Vol. 20, No. 4, 1997, pp. 715–720.

[5]Wu, A. K., and Miele, A., "Sequential Conjugate Gradient-Restoration Algorithm for Optimal Control Problems with Non-Differential Constraints and General Boundary Conditions, Part I," *Optimal Control Applications and Methods*, Vol. 1, No. 1, 1980, pp. 69–88.

[6]Gonzalez, S., and Rodrigues, S., "Modified Quasilinearization Algorithm for Optimal Control Problems with Nondifferential Constraints and General Boundary Conditions," *Journal of Optimization Theory and Applications*, Vol. 50, No. 1, 1986, pp. 109–128.

Multiple Model-Based Terminal Guidance Law

Ilan Rusnak*
RAFAEL, Ministry of Defense, 31021 Haifa, Israel

I. Introduction

THERE are continuing efforts to improve the performance of guidance laws for the terminal phase of a missile intercepting maneuvering targets. More detailed models have been introduced for derivation of guidance laws with improved performance with respect to the classical proportional navigation. The inclusion of the stochastic nature of the measurements led to the introduction of Kalman filters into guidance.[1,2] The inclusion of the missile dynamics and target maneuver, by the use of the optimal control theory, was considered in Refs. 1, 3, and 4. When the target acceleration is unknown the shaping filter was used in Ref. 1 to account for the target's maneuver. The missile acceleration constraint has been dealt with in Ref. 3. The differential games approach has been presented in Refs. 5–7.

Here we concentrate on more detailed modeling of the target maneuver. Namely, the contribution of this paper is the application of the multiple model-based approach to the derivation of a guidance law for the terminal phase of a missile intercepting a maneuvering target. We consider the multiple model adaptive control (MMAC) architecture[8,9] and the multiple model adaptive estimation (MMAE)-based control architecture.[10] These architectures are suboptimal, feasible algorithms for control of uncertain systems. They have been applied to control of uncertain systems with success.[11]

The main objective is to assess the improvement in performance that can be achieved by application of the multiple model-based algorithm to the derivation of the guidance law: the multiple model-based guidance law (MMGL). The comparison between the guidance law based on the shaping filter[1] and the MMGL is performed on a common basis. By common basis we mean that the information available for both approaches is identical.

The guidance law based on the shaping filter is linear and time-varying. The MMGL is time-varying and nonlinear. A simple example is presented to identify the improvement and to keep the numerical effort affordable, as it increases rapidly with the number of model hypotheses. In the example we assume a missile with an instantaneous time response autopilot, guided against a maneuvering target that performs a step maneuver whose initiation instant is uniformly distributed over the short terminal intercept period. The simulations show that the MMGL has improved performance, in term of a smaller miss distance, with respect to the guidance law based on the shaping filter approach.

II. Statement of the Problem

The following is the problem of control on an nth-order stochastic linear discrete-time uncertain system on finite time.[8] The system is specified by the following model:

$$x(i+1) = A(\theta)x(i) + m(\theta, i) + b(\theta)u(i) + v(i), \qquad x(0) = x_0$$

$$y(i) = c(\theta)x(i) + w(i), \qquad i = 0, 1, 2, \ldots, N-1 \quad (1)$$

where $x(i) \in R^n$ is the state; $u(i) \in R^1$ is the input and $y(i) \in R^1$ is the measured output; $A(\theta) \in R^{n \times n}$ and $b(\theta)$, $c(\theta)^T \in R^n$; and $m(\theta, i) \in R^n$ is an external deterministic input for a given θ. The sequences $v(i)$ and $w(i) \in R^1$ are mutually independent excitation and observation noise processes, respectively. They are zero-mean white Gaussian sequences with covariances $E[v(i)v(j)^T] = V(j, \theta)\delta_{ij}$ and $E[w(i)w(j)^T] = W(j, \theta)\delta_{ij}$. The initial state vector x_0 is Gaussian and independent of $v(i)$ and $w(i)$ for $i \geq 0$ and has a priori probability density $p[x(0)]$ with mean $\bar{x}_0$ and covariance Q_0.

Received 5 May 1999; revision received 27 December 1999; accepted for publication 31 December 1999.

*Senior Research Scientist, P.O. Box 2250. Member AIAA.